SUPPLEMENTARY MATERIAL

Numerical models based on a minimal set of sarcolemmal electrogenic proteins and an intracellular Ca^{2+}clock generate robust, flexible, and energy-efficient cardiac pacemaking

Victor A. Maltsev and Edward G. Lakatta

SUPPLEMENTAL FIGURES

SUPPLEMENTAL TABLES

MODEL EQUATIONS

REFERENCES CITED IN THE ONLINE SUPPLEMENT

SUPPLEMENTAL FIGURES

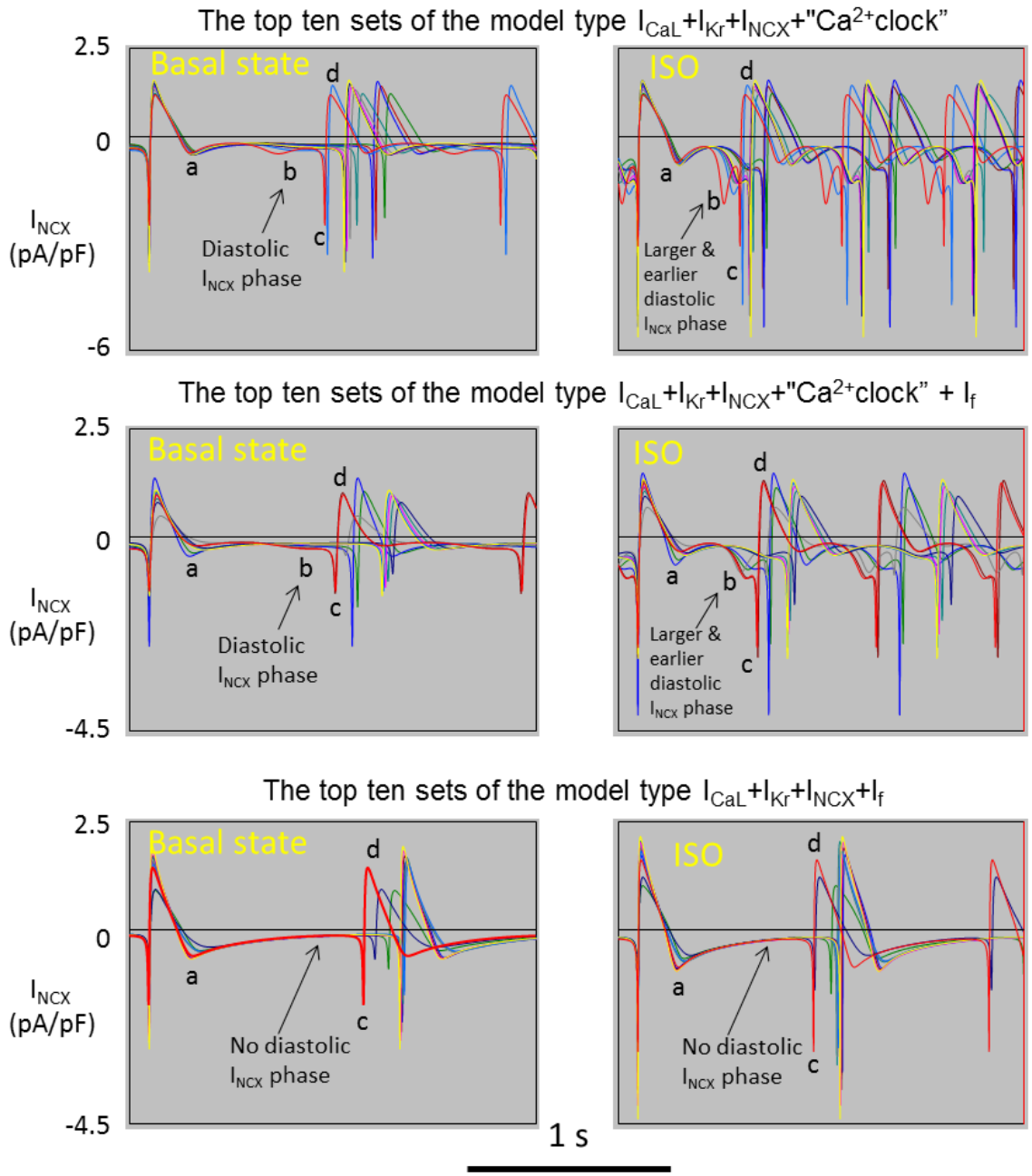

Supplemental Figure S1. Mechanisms of flexibility in the coupled-clock models vs. M-clock models. Dynamics of I_{NCX} was simulated using the top ten model sets for each of three model types (indicated at the panels' top) in Basal State and in the presence of β-AR stimulation (ISO). In ISO tests the diastolic I_{NCX} phase increased in amplitude and occurs earlier in the model sets with Ca^{2+}clock. The diastolic I_{NCX} phase is lacking in pure M-clock sets in Basal State and in ISO test. Parameters of the model sets are given in Table S3. Simulated I_{NCX} traces were synchronized at their most negative values and overlapped. I_{NCX} traces of representative sets used in our mechanistic analyses are shown in red.

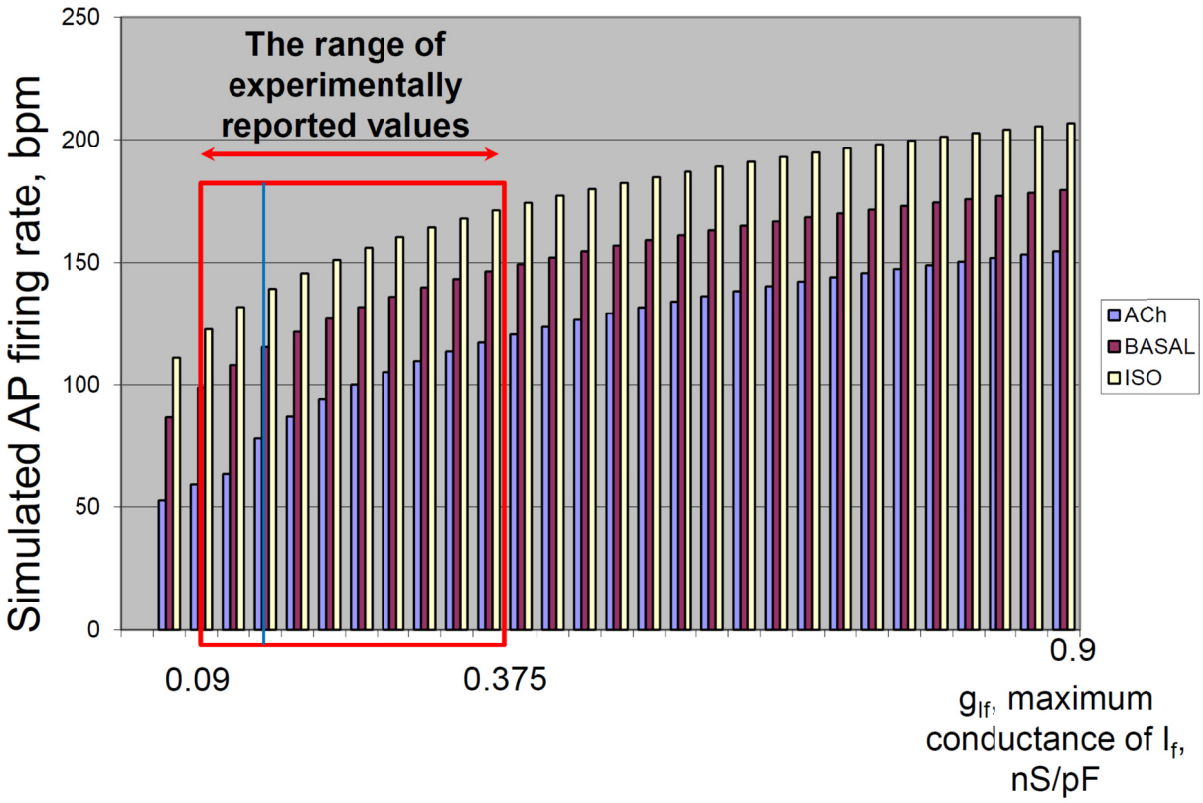

Supplemental Figure S2. A: While I_f serves as an anti-bradycardic mechanism, it limits system flexibility, indicating a fundamental limitation of flexibility of M-clock based pacemaking. Results of simulations using a representative set of a solely M-clock-based pacemaker model type "I_{CaL}+I_{Kr}+I_f+I_{NCX}" (i.e. a 4-component model, lacking Ca^{2+}-clock). When I_f conductance (g_{If} on x-axis) is increased beyond the experimentally measured range, both the minimum rate (ACh, blue bars) and the maximum rate (ISO, yellow bars) increase concurrently, so that the relative rate flexibility is compromised. The double head arrow shows the range of I_f conductance (g_{If}) that simulates the respective range of If densities measured experimentally [1] (see main text Figure 1C). Specific parameters (other than g_{If}) for this model set are given in Table S3 (highlighted in the section I_{CaL}+I_{Kr}+I_f+I_{NCX})

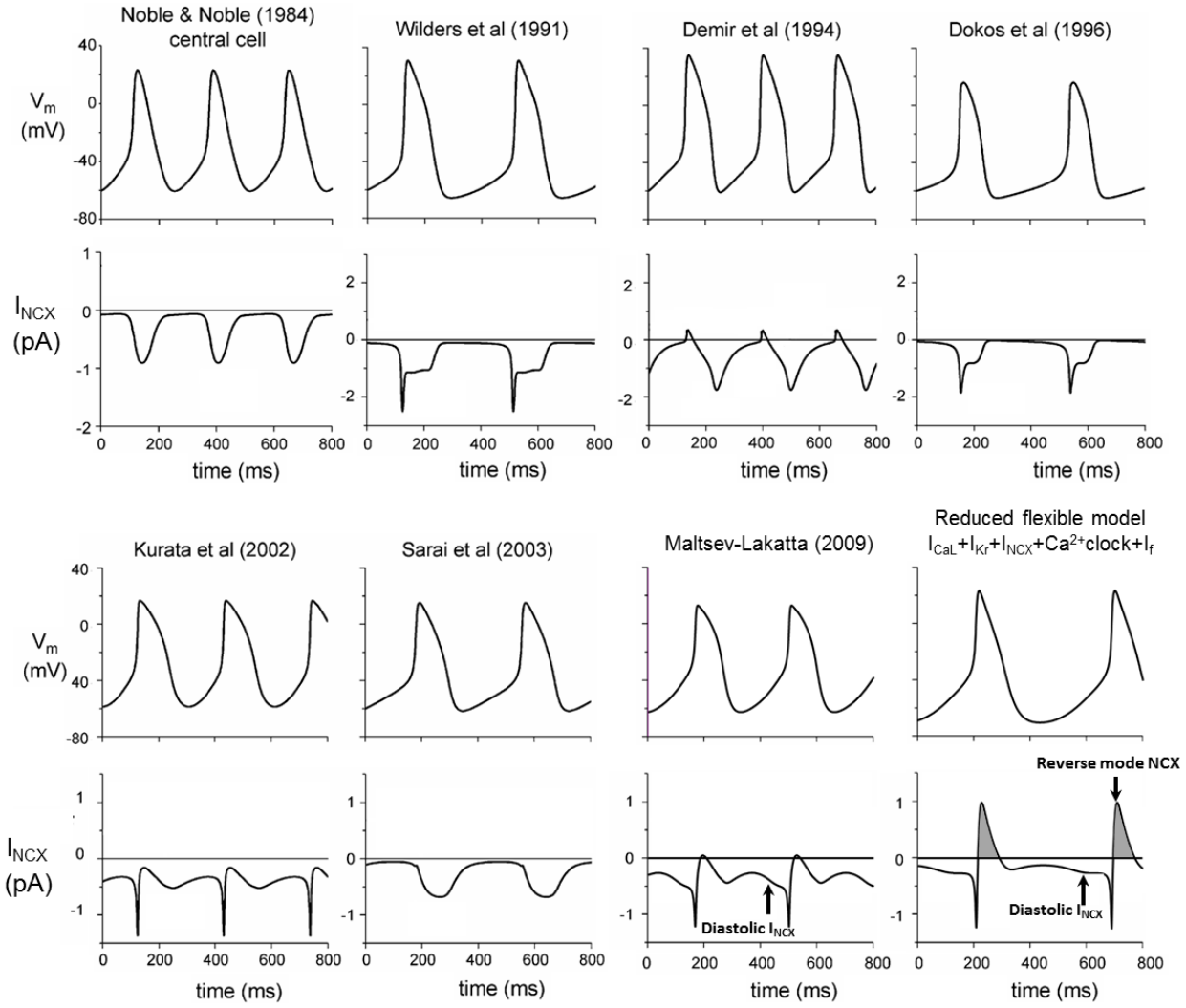

Supplemental Figure S3. Comparison of I_{NCX} dynamics in different pacemaker cell models. Only models that feature Ca^{2+} clock, e.g. Maltsev-Lakatta model (2009) and "$I_{CaL}+I_{Kr}+I_{NCX}+Ca^{2+}clock+I_f$" model, exhibit substantial increase in diastolic I_{NCX}. Also, our new flexible models, such as "$I_{CaL}+I_{Kr}+I_{NCX}+Ca^{2+}clock+I_f$", lacking I_{bNa} and I_{st}, feature a unique phase of the reverse mode NCX, illustrated in gray. All simulations of V_m and I_{NCX} (except "Maltsev-Lakatta 2009" and "Reduced flexible model") are modified panels of 2007 Wilders review [2].

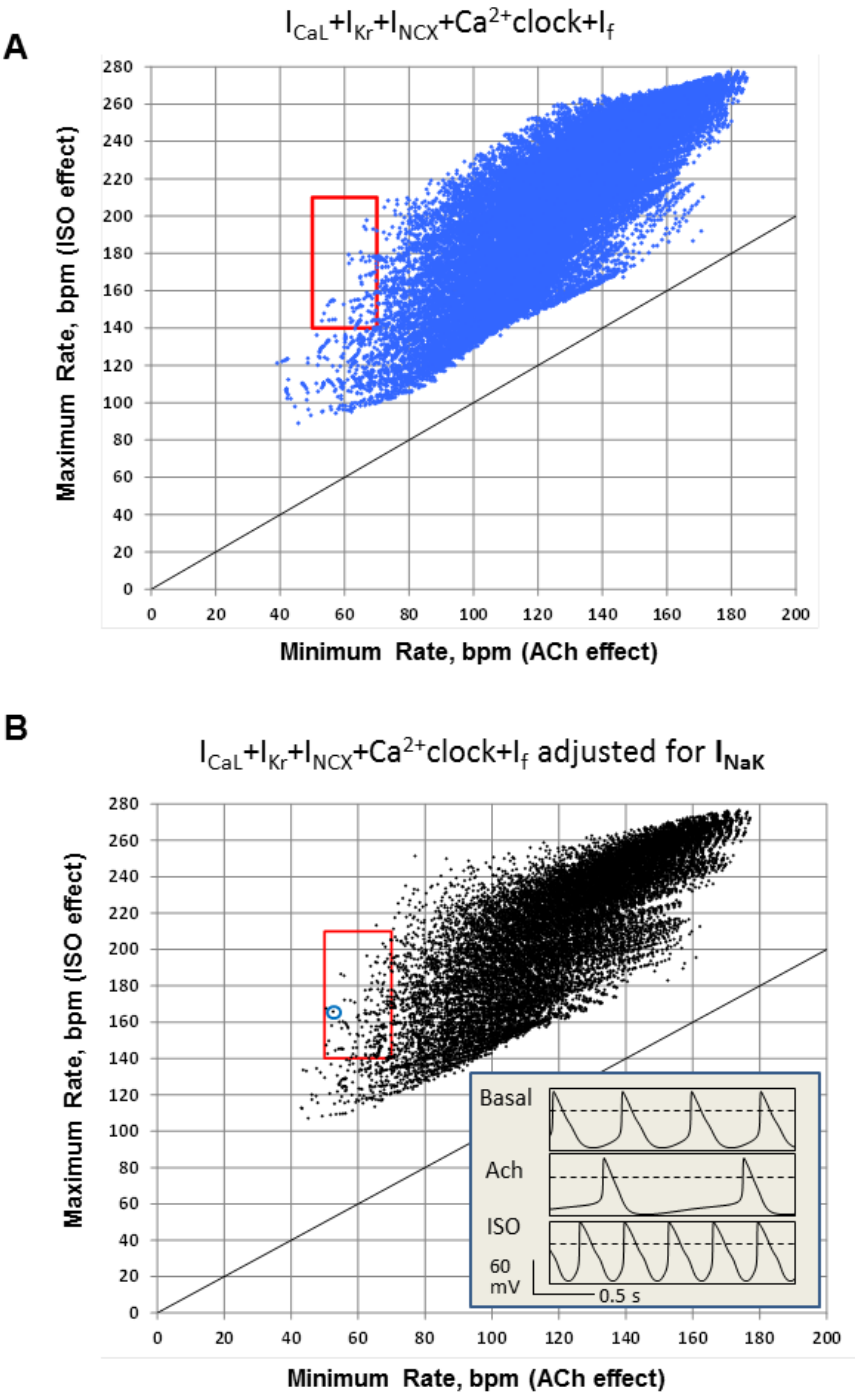

Supplemental Figure S4. The 5-parameter model type "$I_{CaL}+I_{Kr}+I_{NCX}+Ca^{2+}clock+I_f$" remains flexible after its adjustment for outward current produced Na^+/K^+ ATPase (I_{NaK}). Shown are the results of sensitivity analysis of this model with two settings (A) without I_{NaK}, and (B) with I_{NaK} of fixed maximum density ($I_{NaK,max}$=0.9 pA/pF). The results of the parametric analysis are given in main text Table 1 (models #8 and 8b). Inset shows an example of AP simulations for a physiologically flexible set with adjusted I_{KNa} within blue circle (set#4 of the top 10, Table S3).

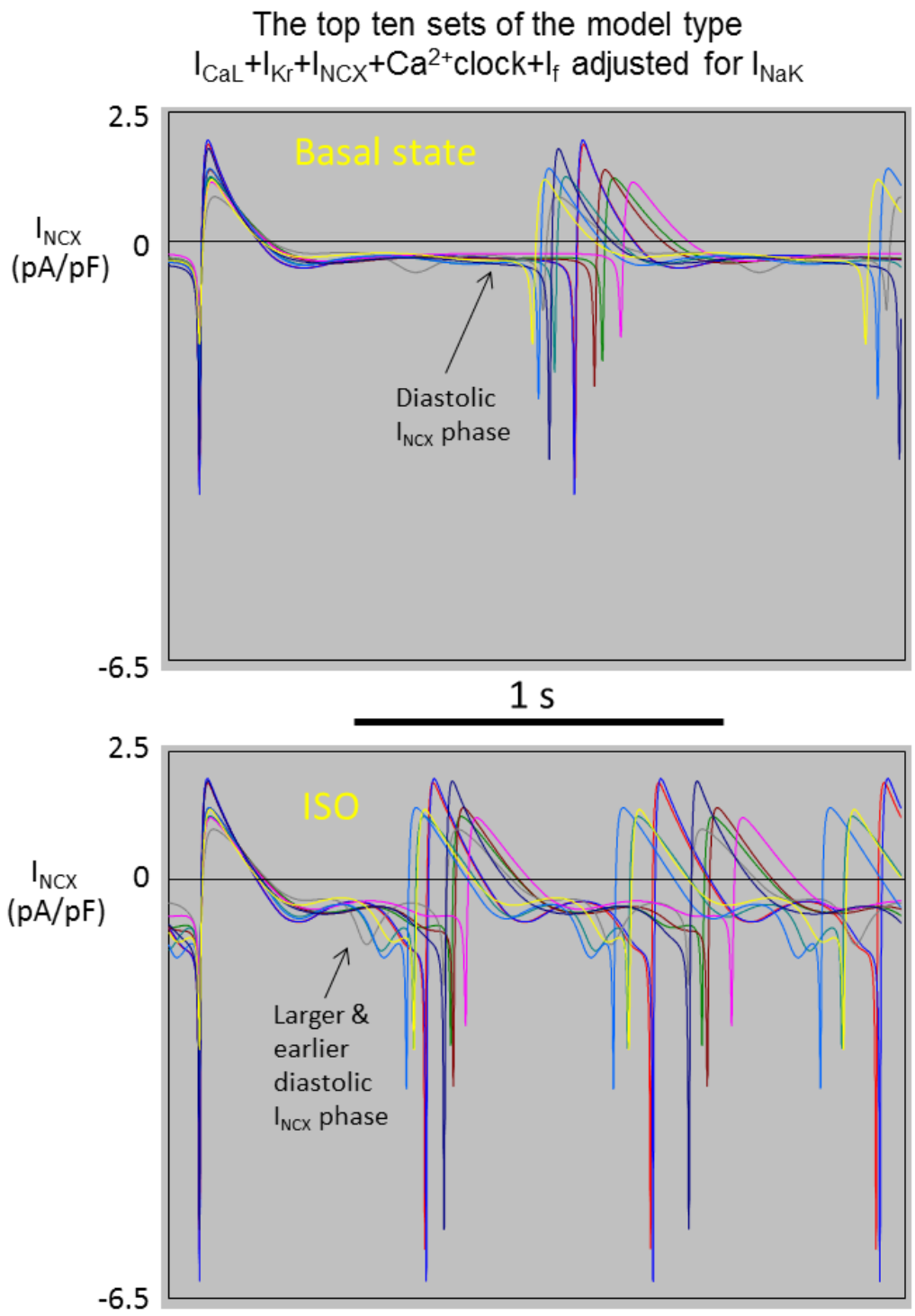

Supplemental Figure S5. Robust and flexible model "$I_{CaL}+I_{Kr}+I_{NCX}+Ca^{2+}clock+I_f$" adjusted for outward current produced by Na^+/K^+ ATPase (I_{NaK}) exhibits the same mechanism of rate increase in the presence of β-AR stimulation (ISO) via an earlier and larger diastolic I_{NCX}. Shown are simulations of I_{NCX} dynamic for the top ten model sets of this model type that included I_{NaK} (see Table S3 for model set parameters) in the Basal state and in ISO test. Simulated I_{NCX} traces were synchronized at their most negative values and overlapped.

SUPPLEMENTAL TABLES

Supplement Table S1. Model variables: description and initial values. All initial values were taken from our prior studies [3,4].

#	Variable	Description	Initial value
		Ca^{2+} cycling	
y_1	Ca_i	[Ca^{2+}] in myoplasm, mM	0.0001
y_2	Ca_{sub}	[Ca^{2+}] in submembrane space, mM	0.000223
y_3	Ca_{jSR}	[Ca^{2+}] in the junctional SR (jSR), mM	0.029
y_4	Ca_{nSR}	[Ca^{2+}] in the network SR (nSR), mM	1.35
y_5	f_{TC}	Fractional occupancy of the troponin-Ca^{2+} site by Ca^{2+} in myoplasm	0.02
y_6	f_{TMC}	Fractional occupancy of the troponin-Mg^{2+} site by Ca^2 in myoplasm	0.22
y_7	f_{TMM}	Fractional occupancy of the troponin-Mg^{2+} site by Mg^{2+} in myoplasm	0.69
y_8	f_{CMi}	Fractional occupancy of calmodulin by Ca^{2+} in myoplasm	0.042
y_9	f_{CMs}	Fractional occupancy of calmodulin by Ca^{2+} in submembrane space	0.089
y_{10}	f_{CQ}	Fractional occupancy of calsequestrin by Ca^{2+} in junctional SR	0.032
y_{11}	R	RyR reactivated (closed) state	0.7499955
y_{12}	O	RyR open state	$3.4 \cdot 10^{-6}$
y_{13}	I	RyR inactivated state	$1.1 \cdot 10^{-6}$
y_{14}	RI	RyR RI state	0.25
		Electrophysiology	
y_{15}	V_m	Membrane potential, mV	-65
y_{16}	d_L	I_{CaL} activation	0
y_{17}	f_L	I_{CaL} voltage-dependent inactivation	1
y_{18}	f_{Ca}	I_{CaL} Ca^{2+} dependent inactivation	1
y_{19}	p_{aF}	I_{Kr} fast activation	0
y_{20}	p_{aS}	I_{Kr} slow activation	0
y_{21}	p_i	I_{Kr} inactivation	1
y_{22}	y	I_f activation	1
y_{23}	a	I_{KACh} activation	1
y_{24}	d_T	I_{CaT} activation	0
y_{25}	f_T	I_{CaT} inactivation	1

Supplement Table S2. Specific parameter variations in sensitivity analysis to create model sets and specific changes of the model parameters to test autonomic modulation in each model set.

Parameter name (and its variable)	Parameter value in the original ML model [3]	Gradations of the parameter to create model sets	Change of the basal value (100%) of a set via autonomic modulation, ChR to β-AR stimulation
Maximal I_{CaL} conductance (g_{CaL})	$g_{CaL,basal}$ = 0.58 nS/pF	0.116 to 1.16 nS/pF (in 10 gradations)	-16.3% to +75% [5-7]
I_f voltage activation ($V_{½,If}$)	$V_{½,If,basal}$ = -64 mV	-64 mV (not varied)	-5.8 mV to +7.8 mV [6,8,9]
Maximal I_f conductance (g_{If})	g_{If} = 0.15 nS/pF	0.03 to 0.3 nS/pF (in 10 gradations)	Unchanged
Maximal I_{Kr} conductance (g_{Kr})	$g_{Kr,basal}$ = 0.08114 nS/pF	0.016228 to 0.16228 nS/pF (in 10 gradations)	0% to +50% [10]
Maximal I_{NCX} (k_{NCX})	k_{NCX} = 187.5 pA/pF	37.5 to 375 pA/pF (in 10 gradations)	Unchanged
Maximul SR Ca^{2+} pumping rate (P_{up})	$P_{up,basal}$ = 12 mM/s	2 to 24 mM/s (in 10 gradations)	-36.7% to +100% [4]
Maximal I_{KACh} conductance (g_{KAch})	g_{KAch}=0.142418 18 nS/pF [4]	0.028483636 to 0.28483636 nS/pF (in 10 gradations)	I_{KACh}=0 for basal state and β-AR stimulation; $I_{KACh}=a\cdot g_{KACh}\cdot(V_m - E_K)$ for ChR stimulation
Maximal I_{CaT} conductance (g_{CaT})	g_{CaT} = 0.1832 nS/pF	0.03664 to 0.3664 nS/pF (in 10 gradations)	Unchanged

Supplemental Table S3. The top 10 sets. Specific parameters and key characteristics of APs summarized for the top 10 model sets for each of 4 model types that were used in our mechanistic analyses. These sets were the top ten with respect to their relative flexibility [column "rel.flex%" = 100%* (IsoBPM- AchBPM)/ AchBPM]) and had a minimum rate of 50 to 70 bpm (column AchBPM) and AP amplitudes (columns with "Ampl") of more than 80 mV. The AP firing rates (BPM) are given in bpm; AP amplitudes (Amp) in mV; Maximum Diastolic Potential (MDP) in mV; Maximum SR Ca^{2+} pumping rate (Pup) in mM/s; ion current conductances gCaL,gIf, gKr in nS/pF; NCX current coefficient (kNCX) in pA/pF. "Ach" indicates results of ACh test, "Iso" for ISO test, "bas" for Basal state test. Highlighted are the model sets that were used as representative examples in illustrations in our mechanistic analyses.

The top ten sets for model "$I_{CaL}+I_{Kr}+I_{NCX}+I_f$"

#	AchBPM	basBPM	IsoBPM	Pup	gCaL	gIf	gKr	kNCX	basAmpl	basMDP	AchAmpl	AchMDP	IsoAmpl	IsoMDP	rel.flex%
1	56.028	97.017	119.88	0	0.812	0.09	0.0811	112.5	105.35	-72.1	102.7	-72.86	114.3	-75.83	113.96
2	**63.789**	**108.09**	**131.9**	**0**	**0.928**	**0.12**	**0.0974**	**225**	**105.78**	**-72.5**	**103.4**	**-73.25**	**114.3**	**-76**	**106.78**
3	54.805	91.743	113.27	0	1.16	0.06	0.1136	225	110.7	-74.8	109.1	-75.44	117.7	-77.78	106.68
4	56.117	92.116	113.82	0	1.16	0.06	0.1136	262.5	110.18	-74.5	108.6	-75.15	117.3	-77.55	102.83
5	57.372	91.519	116.3	0	0.696	0.06	0.0649	375	94.836	-65.6	92.27	-66.35	106.7	-70.88	102.71
6	57.507	91.324	115.98	0	0.696	0.06	0.0649	337.5	95.258	-65.9	92.71	-66.6	107	-71.06	101.68
7	56.891	92.407	114.25	0	1.16	0.06	0.1136	300	109.74	-74.2	108.1	-74.91	117	-77.35	100.82
8	57.665	91.095	115.57	0	0.696	0.06	0.0649	300	95.757	-66.2	93.24	-66.91	107.4	-71.28	100.42
9	65.524	102.88	131	0	0.464	0.12	0.0487	187.5	85.352	-61.5	80.9	-62.27	99.64	-67.44	99.927
10	57.405	92.635	114.59	0	1.16	0.06	0.1136	337.5	109.38	-74	107.8	-74.7	116.8	-77.19	99.617

The top ten sets for model "$I_{CaL}+I_{Kr}+I_{NCX}+Ca^{2+}$clock"

#	AchBPM	basBPM	IsoBPM	Pup	gCaL	gIf	gKr	kNCX	basAmpl	basMDP	AchAmpl	AchMDP	IsoAmpl	IsoMDP	rel.flex%
1	53.691	102.46	184.93	9.6	1.044	0	0.0811	262.5	111.42	-74.9	109.1	-74.61	118.5	-78.47	244.43
2	52.551	98.636	179.72	9.6	1.044	0	0.0811	187.5	111.52	-75.5	109.7	-75.27	118.2	-78.66	241.99
3	54.348	103.96	183.68	9.6	1.044	0	0.0811	337.5	111.52	-74.6	108.8	-74.19	119.1	-78.46	237.97
4	**67.416**	**132.16**	**226.97**	**16.8**	**1.16**	**0**	**0.1136**	**187.5**	**116.07**	**-79.7**	**114.5**	**-79.59**	**120.6**	**-81.08**	**236.67**
5	59.901	111.79	200.84	12	1.16	0	0.0974	187.5	114.39	-77.7	112.8	-77.52	119.8	-79.95	235.29
6	61.747	115.56	206.58	12	1.16	0	0.0974	225	114.37	-77.4	112.6	-77.2	119.9	-79.81	234.56
7	62.969	117.5	207.36	12	1.16	0	0.0974	262.5	114.44	-77.2	112.5	-76.96	120.2	-79.78	229.3
8	68.174	130.14	221.28	14.4	1.044	0	0.0974	300	114.36	-77.8	111.9	-77.38	120.2	-80.2	224.58
9	63.837	118.52	206.65	12	1.16	0	0.0974	300	114.56	-77.1	112.4	-76.77	120.5	-79.79	223.72
10	64.478	119.07	205.37	12	1.16	0	0.0974	337.5	114.69	-77	112.3	-76.61	120.8	-79.81	218.51

Supplemental Table S3, continued…

The top ten sets for model "$I_{CaL}+I_{Kr}+I_{NCX}+Ca^{2+}clock+I_f$"

#	AchBPM	basBPM	IsoBPM	Pup	gCaL	gIf	gKr	kNCX	basAmpl	basMDP	AchAmpl	AchMDP	IsoAmpl	IsoMDP	rel.flex%
1	**66.09**	**124.57**	**194.3**	**14.4**	**0.348**	**0.03**	**0.0487**	**337.5**	**93.753**	**-70.5**	**82.56**	**-68.39**	**108.3**	**-76.67**	**193.99**
2	61.412	111.44	174.62	9.6	0.696	0.03	0.0811	187.5	106.69	-75.4	102.3	-74.74	115.8	-79.3	184.34
3	62.312	114.42	176.83	9.6	0.812	0.03	0.0974	300	110.29	-76.5	105.8	-75.97	118.6	-80.02	183.78
4	68.894	124.92	192.99	14.4	0.348	0.03	0.0487	375	93.953	-70.5	83.21	-68.38	108.8	-76.69	180.13
5	54.815	97.253	152.25	7.2	0.464	0.03	0.0487	187.5	93.815	-67.8	87.84	-66.76	107.5	-74.33	177.75
6	65.03	118.12	180.61	14.4	0.232	0.06	0.0325	150	77.235	-63.4	63.39	-61.16	94.3	-70.51	177.73
7	55.507	98.401	153.98	7.2	0.464	0.03	0.0487	225	93.666	-67.4	87.37	-66.33	107.7	-74.17	177.41
8	55.962	99.182	154.64	7.2	0.464	0.03	0.0487	262.5	93.582	-67.2	87	-66	108	-74.07	176.33
9	53.662	95.39	147.84	7.2	0.464	0.03	0.0487	150	94.095	-68.2	88.46	-67.34	107.4	-74.59	175.5
10	56.288	99.709	154.86	7.2	0.464	0.03	0.0487	300	93.532	-67	86.7	-65.74	108.3	-73.98	175.12

The top ten sets for model "$I_{CaL}+I_{Kr}+I_{NCX}+Ca^{2+}clock+I_f$" adjusted for I_{NaK} ($I_{NaK,max}$=0.9 pA/pF)

#	AchBPM	basBPM	IsoBPM	Pup	gCaL	gIf	gKr	kNCX	basAmpl	basMDP	AchAmpl	AchMDP	IsoAmpl	IsoMDP	rel.flex%
1	54.865	112.09	186.51	9.6	1.16	0.03	0.0487	337.5	108.04	-71	105.9	-71.24	115.1	-74.35	239.94
2	50.418	104.48	167.48	9.6	1.044	0.03	0.0325	150	99.811	-65	101.4	-68.13	104.3	-65.64	232.18
3	55.876	112.25	185.53	9.6	1.16	0.03	0.0487	375	108.18	-70.9	105.8	-71.09	115.4	-74.4	232.04
4	52.592	106.54	165.75	9.6	1.044	0.03	0.0325	187.5	99.316	-64.2	100.9	-67.55	103.8	-64.88	215.16
5	62.689	118.52	196.5	12	1.16	0.03	0.0487	150	108.11	-72.5	107.6	-73.5	113.2	-74	213.45
6	55.957	122.49	172.19	21.6	0.696	0.06	0.0325	112.5	98.149	-69.4	98.31	-72.46	104.1	-69.88	207.72
7	52.129	99.892	158.1	7.2	0.812	0.06	0.0325	150	96.967	-64.9	95.88	-66.43	105.3	-68.35	203.29
8	67.446	124.12	203.22	12	1.16	0.03	0.0487	187.5	107.97	-72.1	107.3	-72.99	113.1	-73.76	201.31
9	57.751	120.26	171.97	12	0.928	0.03	0.0325	375	99.454	-64.1	100.3	-67.97	103.6	-63.85	197.78
10	65.938	126.37	195.95	12	0.58	0.09	0.0325	225	95.029	-66.8	90.82	-67.68	104	-69.53	197.17

MODEL EQUATIONS

All model equations were taken from our previously published version of a "Basal State" model of rabbit SANC [4]. Many ion current formulations were excluded as described in the main text and summarized in the Table 1. We tested behavior of substantial number of model sets with their specific ion current densities and the SR Ca^{2+} pumping rate given in supplemental Table S2 (3rd column). The specific changes of the model parameters in our simulations of either β-AR stimulation or ChR stimulation are summarized in Table S2 (4th column) and also given below within the model equations. The specific values of model parameter sets that reproduced human heart rate variability are given in supplemental Excel files (one file for each model type). Specific parameter values of "the top 10" model sets are given in Table S3.

PARAMETERS

Fixed ion concentrations, mM

$Ca_o = 2$: Extracellular Ca^{2+} concentration.
$K_o = 5.4$: Extracellular K^+ concentration.
$K_i = 140$: Intracellular K^+ concentration.
$Na_o = 140$: Extracellular Na^+ concentration.
$Na_i = 10$: Intracellular Na^+ concentration.
$Mg_i = 2.5$: Intracellular Mg^{2+} concentration.

Cell compartments

$C_m = 32$ pF: Cell electric capacitance.
$L_{cell} = 70$ μm: Cell length.
$R_{cell} = 4$ μm: Cell radius.
$L_{sub} = 0.02$ μm: Distance between jSR and surface membrane (submembrane space).
$V_{cell} = \pi \cdot R_{cell}^2 \cdot L_{cell} = 3.5185838$ pL: Cell volume.
$V_{sub} = 2\pi \cdot L_{sub} \cdot (R_{cell} - L_{sub}/2) \cdot L_{cell} = 0.035097874$ pL: Submembrane space volume.
$V_{jSR\_part} = 0.0012$: Part of cell volume occupied by junctional SR.
$V_{jSR} = V_{jSR\_part} \cdot V_{cell}$: Volume of junctional SR (Ca^{2+} release store).
$V_{i\_part} = 0.46$: Part of cell volume occupied with myoplasm.
$V_i = V_{i\_part} \cdot V_{cell} - V_{sub}$: Myoplasmic volume.
$V_{nSR\_part} = 0.0116$: Part of cell volume occupied by network SR.
$V_{nSR} = V_{nSR\_part} \cdot V_{cell}$: Volume of network SR ($Ca^{2+}$ uptake store).

The Nernst equation and electric potentials, mV

$E_X = (RT/F) \cdot \ln([X]_o/[X]_i) = E_T \cdot \ln([X]_o/[X]_i)$, where
F = 96485 C/M is Faraday constant,
T = 310.15 K˚ is absolute temperature for 37˚C,
R = 8.3144 J/(M·K˚) is the universal gas constant,
E_T is "RT/F" factor = 26.72655 mV,
and $[X]_o$ and $[X]_i$ are concentrations of an ion "X" out and inside cell, respectively.
$E_{Na} = E_T \cdot \ln(Na_o/Na_i)$: Equilibrium potential for Na^+.

$E_K = E_T \cdot \ln(K_o/K_i)$: Equilibrium potential for K^+.
$E_{CaL} = 45$: Apparent reversal potential of I_{CaL}.

Sarcolemmal ion current types and their parameter values
Note: See Table S2 for different specific values of the following parameters that were tested in the present study: $g_{CaL,basal}$ g_{If}, $V_{½,If,basal}$, $g_{Kr,basal}$, k_{NCX}, $P_{up,basal}$, g_{KAch}, and g_{CaT}.

I_{CaL}: L-type Ca^{2+} current.
Steady-state activation parameters: $V_{½,d}$ =-13.5 mV; K_d =6 mV.
Steady-state inactivation parameters: $V_{½,f}$ =-35 mV; K_f =7.3 mV.
$K_{mfCa} = 0.00035$ mM: Dissociation constant of Ca^{2+} -dependent I_{CaL} inactivation.
$\beta_{fCa} = 60$ $mM^{-1} \cdot ms^{-1}$: Ca^{2+} association rate constant for I_{CaL}.
$\alpha_{fCa} = 0.021$ ms^{-1} : Ca^{2+} dissociation rate constant for I_{CaL}
$b_{CaL,max} = 0.31$: maximum ACh-induced inhibition of I_{CaL}.

I_f: Hyperpolarization-activated current.
$V_{If,1/2,basal}$: half activation voltage for I_f current in the basal state.
$s_{max} = -7.2$ mV: maximum ACh-induced shift of I_f half activation voltage.
$n_f = 0.69$ and $K_{0.5,f} = 12.6$ nM: Michaelis-Menton parameters for ACh modulation of I_f.

I_{Kr}: Delayed rectifier K^+ current rapid component.

I_{NCX}: Na^+/Ca^{2+} exchanger (NCX) current.
$K_{1ni} = 395.3$: intracellular Na^+ binding to first site on NCX.
$K_{2ni} = 2.289$: intracellular Na^+ binding to second site on NCX.
$K_{3ni} = 26.44$: intracellular Na^+ binding to third site on NCX.
$K_{1no} = 1628$: extracellular Na^+ binding to first site on NCX.
$K_{2no} = 561.4$: extracellular Na^+ binding to second site on NCX.
$K_{3no} = 4.663$: extracellular Na^+ binding to third site on NCX.
$K_{ci} = 0.0207$: intracellular Ca^{2+} binding to NCX transporter.
$K_{co} = 3.663$: extracellular Ca^{2+} binding to NCX transporter.
$K_{cni} = 26.44$: intracellular Na^+ and Ca^{2+} simultaneous binding to NCX.
$Q_{ci} = 0.1369$: intracellular Ca^{2+} occlusion reaction of NCX.
Q_{co}=0: extracellular Ca^{2+} occlusion reaction of NCX.
$Q_n = 0.4315$: Na^+ occlusion reactions of NCX.

I_{KACh}: Acetylcholine-activated K^+ current; I_{KACh} =0, when [ACh]=0.

I_{CaT}: T-type Ca^{2+} current.

I_{NaK}: Na^+/K^+ pump current. I_{NaKmax}=0 in all models, except model #8b (main text Table 1), in which $I_{NaKmax} = 0.9$ pA/pF.
$K_{mKp} = 1.4$ mM: Half-maximal K_o for I_{NaK}.
$K_{mNap} = 14$ mM: Half-maximal Na_i for I_{NaK}.

Ca^{2+} diffusion

τ_{difCa} = 0.04 ms: Time constant of Ca^{2+} diffusion from the submembrane to myoplasm.
τ_{tr} = 40 ms: Time constant for Ca^{2+} transfer from the network to junctional SR.

SR Ca^{2+} ATPase function

$K_{up} = 0.6 \cdot 10^{-3}$ mM: Half-maximal Ca_i for Ca^{2+} uptake in the network SR.
$P_{up,basal}$ = 0.0144 mM/ms: Rate constant for Ca^{2+} uptake by the Ca^{2+} pump in the network SR (Please note that while we performed j_{up} computations in mM/ms, our results of parametric sensitivity analysis in main text and Tables are presented in mM/s).

RyR function

$k_{oCa} = 10\ mM^{-2} \cdot ms^{-1}$; $k_{om} = 0.06\ ms^{-1}$; $k_{iCa} = 0.5\ mM^{-1} \cdot ms^{-1}$; $k_{im} = 0.005\ ms^{-1}$; $EC_{50\_SR} = 0.45$ mM; $k_s = 250 \cdot 10^3\ ms^{-1}$; $MaxSR = 15$; $MinSR = 1$; $HSR = 2.5$;

Ca^{2+} and Mg^{2+} buffering

k_{bCM}=0.542 ms^{-1}: Ca^{2+} dissociation constant for calmodulin.
k_{bCQ}=0.445 ms^{-1}: Ca^{2+} dissociation constant for calsequestrin.
k_{bTC}=0.446 ms^{-1}: Ca^{2+} dissociation constant for the troponin-Ca^{2+} site.
k_{bTMC}=0.00751 ms^{-1}: Ca^{2+} dissociation constant for the troponin-Mg^{2+} site.
k_{bTMM}=0.751 ms^{-1}: Mg^{2+} dissociation constant for the troponin-Mg^{2+} site.
k_{fCM}=227.7 $mM^{-1} \cdot ms^{-1}$: Ca^{2+} association constant for calmodulin.
k_{fCQ}=0.534 $mM^{-1} \cdot ms^{-1}$: Ca^{2+} association constant for calsequestrin.
k_{fTC}=88.8 mM/ms: Ca^{2+} association constant for troponin.
k_{fTMC}=227.7 mM/ms: Ca^{2+} association constant for the troponin-Mg^{2+} site.
k_{fTMM}=2.277 mM/ms: Mg^{2+} association constant for the troponin-Mg^{2+} site.
TC_{tot}=0.031 mM: Total concentration of the troponin-Ca^{2+} site.
TMC_{tot}=0.062 mM: Total concentration of the troponin-Mg^{2+} site.
CQ_{tot}=10 mM: Total calsequestrin concentration.
CM_{tot}=0.045 mM: Total calmodulin concentration.

FORMULATIONS: ELECTROPHYSIOLOGY

<u>Membrane potential,</u> V_m (variable y_{15}, see Table S1 for all variables and their initial values)

$$dV_m/dt = -(I_{CaL} + I_f + I_{Kr} + I_{NCX} + I_{CaT} + I_{KACh} + I_{NaK})/C_m$$

<u>Gating variables (y_{16} - y_{25}) and their differential equations</u>

$$dy_i/dt = (y_{i,\infty} - y)/\tau_{yi}$$
$$(y_i = d_L,\ f_L,\ f_{Ca},\ p_{aF},\ p_{aS},\ p_i,\ y,\ a)$$

τ_{yi}: Time constant for a gating variable y_i.
α_{yi} and β_{yi}: Opening and closing rates for channel gating.
$y_{i,\infty}$: Steady-state curve for a gating variable y_i.

Ion currents

L-type Ca^{2+} current (I_{CaL}), based on formulations of Kurata et al. [11] that include Ca^{2+} dependent I_{CaL} inactivation. The fractional block (b_{CaL}) of I_{CaL} by ChR stimulation was adopted from [6] (see Methods for details).

$$I_{CaL}=C_m \cdot g_{CaL} \cdot (V_m - E_{CaL}) \cdot d_L \cdot f_L \cdot f_{Ca}$$
$$d_{L,\infty}=1/\{1+ \exp[-(V_m - V_{½,d})/ K_d]\}$$
$$f_{L,\infty}=1/\{1+\exp[(V_m - V_{½,f})/ K_f]\}$$
$$\alpha_{dL} = -0.02839 \cdot (V_m + 35)/ \{\exp[-(V_m+35)/2.5] - 1\} - 0.0849 \cdot V_m / [\exp(-V_m/4.8) - 1]$$
$$\beta_{dL} = 0.01143 \cdot (V_m - 5)/ \{\exp[(V_m - 5)/2.5] - 1\}$$
$$\tau_{dL} = 1/(\alpha_{dL} + \beta_{dL})$$
$$\tau_{fL} = 0.5*257.1 \cdot \exp\{-[(V_m + 32.5)/13.9]^2\} + 44.3$$
$$f_{Ca,\infty} = K_{mfCa} / (K_{mfCa} + Ca_{sub})$$
$$\tau_{fCa} = f_{Ca,\infty} / \alpha_{fCa}$$

$$g_{CaL} = g_{CaL,basal} \cdot (1 - b_{CaL})$$
in simulations of the effect of ChR stimulation
$$b_{CaL} = b_{CaL,max} \cdot [\text{ACh}]/(K_{0.5,CaL} + [\text{ACh}]) = 0.163 \text{ (for 100 nM [ACh])}$$
or
$g_{CaL} = g_{CaL,basal} \cdot 1.75$ in simulations of the effect of β-AR stimulation by 1 μM ISO[7]

Rapidly activating delayed rectifier K^+ current (I_{Kr}), based on formulations suggested by Zhang et al. [12] and modified by Kurata et al. [11].

$$I_{Kr} = C_m \cdot g_{Kr} \cdot (V_m - E_K) \cdot (0.6 \cdot p_{aF} + 0.4 \cdot p_{aS}) \cdot p_i$$
$$p_{a,\infty} = 1/ \{1 + \exp[-(V_m + 23.2)/10.6]\}$$
$$p_{i,\infty} = 1/ \{1 + \exp[(V_m + 28.6)/17.1]\}$$
$$\tau_{paF} = 0.84655354/[0.0372 \cdot \exp(V_m/15.9) + 0.00096 \cdot \exp(-V_m/22.5)]$$
$$\tau_{paS} = 0.84655354/[0.0042 \cdot \exp(V_m/17.0) + 0.00015 \cdot \exp(-V_m/21.6)]$$
$$\tau_{pi} = 1/[0.1 \cdot \exp(-V_m/54.645) + 0.656 \cdot \exp(V_m/106.157)]$$

$g_{Kr} = g_{Kr,basal}$ in the basal
and in simulations of the effect of ChR stimulation
or
$g_{Kr} = 1.5 \cdot g_{Kr,basal}$ in simulations of the effect of β-AR stimulation by 1 μM ISO [10]

Hyperpolarization-activated, "funny" current (I_f), based on formulations of Wilders at al. [13] and Kurata et al.[11].

$$I_f = I_{fNa} + I_{fK}$$
$$y_\infty = 1/\{1 + \exp[(V_m - V_{If,1/2})/13.5]\}$$
$$\tau_y = 0.7166529/\{\exp[-(V_m + 386.9)/45.302] + \exp[(V_m - 73.08)/19.231]\}$$
$$I_{fNa} = C_m \cdot 0.3833 \cdot g_{If} \cdot (V_m - E_{Na}) \cdot y^2$$
$$I_{fK} = C_m \cdot 0.6167 \cdot g_{If} \cdot (V_m - E_K) \cdot y^2$$

The shift s (in mV) of the I_f activation curve by ChR stimulation was adopted from [6].

$$V_{If,1/2} = V_{If,1/2,basal} + s$$

in simulations of the effect of ChR stimulation by ACh, where

$$s = s_{max}[ACh]^{n_f} /(K_{0.5,f}^{n_f} + [ACh]^{n_f}) = -5.8 \text{ mV (for 100 nM [ACh])}$$

or

$V_{If,1/2} = V_{If,1/2,basal} + 7.8$ mV in simulations of the effect of β-AR stimulation by 1 μM ISO[9]

Na^+-Ca^{2+} exchanger current (I_{NCX}), based on original formulations from Dokos et al. [14].

$$I_{NCX} = C_m \cdot k_{NCX} \cdot (k_{21} \cdot x_2 - k_{12} \cdot x_1) / (x_1 + x_2 + x_3 + x_4)$$
$$d_o = 1+(Ca_o/K_{co})\cdot\{1+\exp(Q_{co}\cdot V_m/E_T)\}+(Na_o/K_{1no})\cdot\{1+(Na_o/K_{2no})\cdot(1+Na_o/K_{3no})\}$$
$$k_{43} = Na_i/(K_{3ni} + Na_i)$$
$$k_{41} = \exp[-Q_n\cdot V_m/(2E_T)]$$
$$k_{34} = Na_o/(K_{3no}+Na_o)$$
$$k_{21} = (Ca_o/K_{co})\cdot\exp(Q_{co}\cdot V_m/E_T)/d_o$$
$$k_{23} = (Na_o/K_{1no})\cdot(Na_o/K_{2no})\cdot(1+Na_o/K_{3no})\cdot \exp[-Q_n\cdot V_m/(2E_T)]/d_o$$
$$k_{32} = \exp[Q_n\cdot V_m/(2E_T)]$$
$$x_1 = k_{34} \cdot k_{41} \cdot (k_{23} + k_{21}) + k_{21} \cdot k_{32} \cdot (k_{43} + k_{41})$$
$$d_i = 1+(Ca_{sub}/K_{ci})\cdot\{1+\exp(-Q_{ci}\cdot V_m/E_T)+Na_i/K_{cni}\}+(Na_i/K_{1ni})\cdot\{1+(Na_i/K_{2ni})\cdot(1+Na_i/K_{3ni})\}$$
$$k_{12} = (Ca_{sub}/K_{ci})\cdot\exp(-Q_{ci}\cdot V_m/E_T)/d_i$$
$$k_{14} = (Na_i/K_{1ni})\cdot(Na_i/K_{2ni})\cdot(1 + Na_i/K_{3ni})\cdot \exp[Q_n\cdot V_m/(2E_T)]/d_i$$
$$x_2 = k_{43}\cdot k_{32} \cdot (k_{14} + k_{12}) + k_{41}\cdot k_{12} \cdot k_{34} + k_{32})$$
$$x_3 = k_{43} \cdot k_{14} \cdot (k_{23} + k_{21}) + k_{12} \cdot k_{23}\cdot(k_{43} + k_{41})$$
$$x_4 = k_{34} \cdot k_{23} \cdot (k_{14} + k_{12}) + k_{21} \cdot k_{14}\cdot(k_{34}+ k_{32})$$

Acetylcholine-activated K^+ current (I_{KACh}), adopted from [15] (Note $I_{KACh} = 0$ when [ACh]=0)

$$I_{KACh} = a \cdot g_{KACh}\cdot (V_m - E_K)$$
$$beta = 0.001 \cdot 12.32/(1+0.0042/[ACh]) \text{ (per ms)}$$
$$alfa = 0.001 \cdot 17\cdot\exp(0.0133\cdot(V_m+40)) \text{ (per ms)}$$
$$a_\infty = beta / (alfa + beta)$$
$$\tau_a = 1/(alfa + beta) \text{ (in ms)}$$

T-type Ca^{2+} current (I_{CaT}), based on formulations suggested by Demir et al., [16] and modified by Kurata et al. [11].

$$I_{CaT} = C_m\cdot g_{CaT} \cdot (V_m - E_{CaT})\cdot d_T\cdot f_T$$
$$d_{T,\infty} = 1/ \{1 + \exp[-(V_m + 26.3)/6.0]\}$$
$$f_{T,\infty} = 1/\{1+ \exp[(V_m + 61.7)/5.6]\}$$
$$\tau_{dT} = 1/\{1.068\cdot\exp[(V_m + 26.3)/30] + 1.068\cdot\exp[-(V_m + 26.3)/30]\}$$
$$\tau_{fT} = 1/\{0.0153\cdot\exp[-(V_m + 61.7)/83.3] + 0.015\cdot\exp[(V_m + 61.7)/15.38]\}$$

Na^+-K^+ pump current (I_{NaK})

$$I_{NaK} = C_m \cdot I_{NaKmax} \cdot \{1+(K_{mKp}/K_o)^{1.2}\}^{-1} \cdot \{1+(K_{mNap}/Na_i)^{1.3}\}^{-1} \cdot \{1+\exp[-(V_m - E_{Na}+120)/30]\}^{-1}$$

FORMULATIONS: Ca^{2+} CYCLING

Ca^{2+} release flux ($j_{SRCarel}$) from SR via RyRs, based on original formulations of Stern et al. [17] and modified by Shannon et al. [18]

$$j_{SRCarel} = k_s \cdot O \cdot (Ca_{jSR} - Ca_{sub})$$
$$k_{CaSR} = MaxSR - (MaxSR - MinSR)/(1 + (EC_{50\_SR}/Ca_{jSR})^{HSR})$$
$$k_{oSRCa} = k_{oCa}/k_{CaSR}$$
$$k_{iSRCa} = k_{iCa} \cdot k_{CaSR}$$
$$dR/dt = (k_{im} \cdot RI - k_{iSRCa} \cdot Ca_{sub} \cdot R) - (k_{oSRCa} \cdot Ca_{sub}^2 \cdot R - k_{om} \cdot O)$$
$$dO/dt = (k_{oSRCa} \cdot Ca_{sub}^2 \cdot R - k_{om} \cdot O) - (k_{iSRCa} \cdot Ca_{sub} \cdot O - k_{im} \cdot I)$$
$$dI/dt = (k_{iSRCa} \cdot Ca_{sub} \cdot O - k_{im} \cdot I) - (k_{om} \cdot I - k_{oSRCa} \cdot Ca_{sub}^2 \cdot RI)$$
$$dRI/dt = (k_{om} \cdot I - k_{oSRCa} \cdot Ca_{sub}^2 \cdot RI) - (k_{im} \cdot RI - k_{iSRCa} \cdot Ca_{sub} \cdot R)$$

Intracellular Ca^{2+} fluxes

Ca^{2+} diffusion flux (j_{Ca_dif}) from submembrane space to myoplasm:

$$j_{Ca\_dif} = (Ca_{sub} - Ca_i)/\tau_{difCa}$$

The rate of Ca^{2+} uptake (pumping) (j_{up}) by the SR, based on formulations of SR Ca^{2+} pump function suggested by Luo and Rudy [19]. The fractional block (b_{up}) of P_{up} by ChR stimulation was described similar to that of I_{CaL} (see above), but $b_{up,max}$ was fitted to experimental curve of phospholamban dephosphorylation [20] (Fig.4A in [4]).

$$j_{up} = P_{up}/(1 + K_{up}/Ca_i)$$

$P_{up} = P_{up,basal} \cdot (1 - b_{up})$ in simulations of the effect of ChR stimulation by 100 nM of ACh, where

$$b_{up} = b_{up,max} \cdot [ACh]/(K_{0.5,up} + [ACh]) = 0.367 \text{ (for 100 nM [ACh])}$$

or

$P_{up} = 2 \cdot P_{up,basal}$ in simulations of the effect of β-AR stimulation by 1 μM ISO[4].

Ca^{2+} flux between (network and junctional) SR compartments (j_{tr}):

$$j_{tr} = (Ca_{nSR} - Ca_{jSR})/\tau_{tr}$$

Ca^{2+} buffering

$$df_{TC}/dt = k_{fTC} \cdot Ca_i \cdot (1 - f_{TC}) - k_{bTC} \cdot f_{TC}$$
$$df_{TMC}/dt = k_{fTMC} \cdot Ca_i \cdot (1 - f_{TMC} - f_{TMM}) - k_{bTMC} \cdot f_{TMC}$$
$$df_{TMM}/dt = k_{fTMM} \cdot Mg_i \cdot (1 - f_{TMC} - f_{TMM}) - K_{bTMM} \cdot f_{TMM}$$
$$df_{CMi}/dt = k_{fCM} \cdot Ca_i \cdot (1 - f_{CMi}) - k_{bCM} \cdot f_{CMi}$$
$$df_{CMs}/dt = k_{fCM} \cdot Ca_{sub} \cdot (1 - f_{CMs}) - k_{bCM} \cdot f_{CMs}$$
$$df_{CQ}/dt = k_{fCQ} \cdot Ca_{jSR} \cdot (1 - f_{CQ}) - k_{bCQ} \cdot f_{CQ}$$

Dynamics of Ca^{2+} concentrations in cell compartments

$$dCa_i/dt = (j_{Ca\_dif} \cdot V_{sub} - j_{up} \cdot V_{nSR})/V_i - (CM_{tot} \cdot df_{CMi}/dt + TC_{tot} \cdot df_{TC}/dt + TMC_{tot} \cdot df_{TMC}/dt)$$
$$dCa_{sub}/dt = j_{SRCarel} \cdot V_{jSR}/V_{sub} - (I_{CaL} + I_{CaT} + I_{bCa} - 2 \cdot I_{NCX})/(2 \cdot F \cdot V_{sub}) - (j_{Ca\_dif} + CM_{tot} \cdot df_{CMs}/dt)$$
$$dCa_{jSR}/dt = j_{tr} - j_{SRCarel} - CQ_{tot} \cdot df_{CQ}/dt$$
$$dCa_{nSR}/dt = j_{up} - j_{tr} \cdot V_{jSR}/V_{nSR}$$

REFERENCES CITED IN THE ONLINE SUPPLEMENT

[1] Honjo H, Boyett MR, Kodama I, Toyama J. Correlation between electrical activity and the size of rabbit sino-atrial node cells. J Physiol 1996;496 (Pt 3):795-808.

[2] Wilders R. Computer modelling of the sinoatrial node. Med Biol Eng Comput 2007;45:189–207.

[3] Maltsev VA, Lakatta EG. Synergism of coupled subsarcolemmal Ca^{2+} clocks and sarcolemmal voltage clocks confers robust and flexible pacemaker function in a novel pacemaker cell model. Am J Physiol Heart Circ Physiol 2009;296:H594-H615.

[4] Maltsev VA, Lakatta EG. A novel quantitative explanation for autonomic modulation of cardiac pacemaker cell automaticity via a dynamic system of sarcolemmal and intracellular proteins. Am J Physiol Heart Circ Physiol 2010;298:H2010-H23.

[5] Zaza A, Robinson RB, DiFrancesco D. Basal responses of the L-type Ca^{2+} and hyperpolarization-activated currents to autonomic agonists in the rabbit sino-atrial node. J Physiol 1996;491 (Pt 2):347-55.

[6] Zhang H, Holden AV, Noble D, Boyett MR. Analysis of the chronotropic effect of acetylcholine on sinoatrial node cells. J Cardiovasc Electrophysiol 2002;13:465-74.

[7] Vinogradova TM, Bogdanov KY, Lakatta EG. beta-Adrenergic stimulation modulates ryanodine receptor Ca^{2+} release during diastolic depolarization to accelerate pacemaker activity in rabbit sinoatrial nodal cells. Circ Res 2002;90:73-9.

[8] DiFrancesco D, Ducouret P, Robinson RB. Muscarinic modulation of cardiac rate at low acetylcholine concentrations. Science 1989;243:669-71.

[9] DiFrancesco D, Tortora P. Direct activation of cardiac pacemaker channels by intracellular cyclic AMP. Nature 1991;351:145-7.

[10] Lei M, Brown HF, Terrar DA. Modulation of delayed rectifier potassium current, iK, by isoprenaline in rabbit isolated pacemaker cells. Exp Physiol 2000;85:27-35.

[11] Kurata Y, Hisatome I, Imanishi S, Shibamoto T. Dynamical description of sinoatrial node pacemaking: improved mathematical model for primary pacemaker cell. Am J Physiol 2002;283:H2074-101.

[12] Zhang H, Holden AV, Kodama I, Honjo H, Lei M, Varghese T, et al. Mathematical models of action potentials in the periphery and center of the rabbit sinoatrial node. Am J Physiol 2000;279:H397-421.

[13] Wilders R, Jongsma HJ, van Ginneken AC. Pacemaker activity of the rabbit sinoatrial node. A comparison of mathematical models. Biophys J 1991;60:1202-16.

[14] Dokos S, Celler B, Lovell N. Ion currents underlying sinoatrial node pacemaker activity: a new single cell mathematical model. J Theor Biol 1996;181:245-72.

[15] Demir SS, Clark JW, Giles WR. Parasympathetic modulation of sinoatrial node pacemaker activity in rabbit heart: a unifying model. Am J Physiol 1999;276:H2221-44.

[16] Demir SS, Clark JW, Murphey CR, Giles WR. A mathematical model of a rabbit sinoatrial node cell. Am J Physiol 1994;266:C832-52.

[17] Stern MD, Song LS, Cheng H, Sham JS, Yang HT, Boheler KR, et al. Local control models of cardiac excitation-contraction coupling. A possible role for allosteric interactions between ryanodine receptors. J Gen Physiol 1999;113:469-89.

[18] Shannon TR, Wang F, Puglisi J, Weber C, Bers DM. A mathematical treatment of integrated Ca dynamics within the ventricular myocyte. Biophys J 2004;87:3351-71.

[19] Luo CH, Rudy Y. A dynamic model of the cardiac ventricular action potential. I. Simulations of ionic currents and concentration changes. Circ Res 1994;74:1071-96.
[20] Lyashkov AE, Vinogradova TM, Zahanich I, Li Y, Younes A, Nuss HB, et al. Cholinergic receptor signaling modulates spontaneous firing of sinoatrial nodal cells via integrated effects on PKA-dependent Ca^{2+} cycling and I_{KACh}. Am J Physiol Heart Circ Physiol 2009;H949-H59.